TM-1152
1183.000
Jan., 1983

A New Look at Displacement Factor and Point of Measurement Corrections in Ionization Chamber Dosimetry.

Miguel Awschalom, Ivan Rosenberg, Randall K. Ten Haken

Fermilab Neutron Therapy Facility, P. O. Box 500, Batavia, IL 60510

ABSTRACT

A new technique is presented for determination of the effective point of measurement when cavity ionization chambers are used to measure the absorbed dose due to ionizing radiation in a dense medium. An algorithm is derived relating the effective point of measurement to the displacement correction factor. This algorithm relates variations of the displacement factor to the radiation field gradient. The technique is applied to derive the magnitudes of the corrections for several chambers in a p(66)Be(49) neutron therapy beam.

KEY WORDS: dosimetry, ionization chambers, point of measurement, displacement correction factor.

Introduction

When a cavity ionization chamber is used to measure the absorbed dose due to ionizing radiation at a point in a medium, it perturbs both the attenuation and the scatter of the radiation by displacing the medium. At depths greater than z_{max} (the depth for maximum dose), this displacement causes an increase in collected ionization over that appropriate for the point in question. To account for this perturbation, a correction must be applied to the absorbed dose calculated from the collected charge. Two schools of thought exist regarding this correction, each internally consistent but apparently incompatible with the other. One method is to multiply the "measured" absorbed dose by a "displacement factor" δ (<1) to obtain the "true" absorbed dose in the absence of the chamber at the point corresponding to the center of the chamber. This factor is known to be dependent on chamber cavity size and it may also be a function of radiation quality,[1-4] but it is thought to be independent of depth, field size, and SSD. The second method assigns the measured dose to a point in the phantom upstream of the center of the chamber. This "effective point of measurement" is generally thought to be displaced a fixed fraction α (<1) of the radius of the chamber cavity, although α could be dependent on the nature of the radiation.[5]

Attempts to derive α from δ or from first principles[3,5] disagree with each other and with experimental or adopted values.[6-9] Derivation of δ from a constant α, on the other hand, necessarily makes δ a function of radiation gradient, i.e., field size and SSD, as pointed out by Dutreix.[5]

Experimental determinations of δ or α have been made in photon and neutron fields[1,6,7,10] by comparing the doses measured with different chambers in the same radiation field. The main weakness of this technique is its reliance on in-air calibrations to determine the relative sensitivities of the various chambers used in phantom. This transfer involves estimating the effects of the wall and the stem of the chamber in the two situations. These corrections are themselves uncertain and they may introduce errors of the same magnitude as the effects under investigation.

In this work, an attempt is made to reconcile the above two approaches in an analytical way by relating δ and α through the gradient of the radiation field. It is shown here that, for high energy photon or neutron beams, where a wide transition region (>5 cm) exists between the depth of maximum dose and the onset of a nearly exponential dose decrease, δ must vary with depth in phantom as well as with field size and SSD. The method is applied to the determination of both α and δ for differently shaped chambers used in a p(66)Be(49)[(a)] neutron therapy beam, without relying on either absolute or relative ionization chamber calibrations.

Analytical Derivation

Let a practical cylindrical or spherical ion chamber of internal cavity radius r be placed with its center at depth z on the central axis of a single ionizing beam (photons or neutrons) in a dense medium (phantom). When exposed to radiation, let its reading be R(z) and its conversion factor to absorbed dose be N, such that N R(z) is the absorbed dose per monitor unit, uncorrected for displacement. Then, to calculate the actual absorbed dose, D(z), two approaches may be used (see Fig. 1):

$$D(z) = N\ R(z)\ \delta(z) \qquad (1)$$

where $\delta(z)$ is the "displacement factor", or

$$D(z-\alpha r) = N\ R(z) \qquad (2)$$

where α is assumed to be a constant smaller than unity.

Thus, for the two approaches to give the same results at all depths, $\delta(z)$ must be a function of αr and D(z):

$$\delta(z) = \frac{D(z)}{D(z-\alpha r)} \qquad (3)$$

As it stands, Eq. 3 includes an unknown function D(z) which has to be obtained separately. This can be done by measuring the same radiation field under identical conditions using a parallel plate ionization chamber (PPIC) with a small gap. Let this parallel plate chamber have an output per monitor unit P(z) at a depth z in the same medium and geometry used for the practical ionization chamber. For a PPIC, no corrections are needed if the depth z of the internal surface of the front electrode is taken as the point of measurement.[6] In other words, the PPIC is assumed to have an output proportional to dose [D(z) = N'P(z)]. Then, the above expression can be rewritten:

$$\delta(z) = \frac{P(z)}{P(z-\alpha r)} \qquad (3a)$$

The relationship between the readings R(z) of a practical chamber and P(z) of the PPIC can be derived using Eq. 1. Let both sets of readings be normalized to unity at a reference depth Z0, i.e., let R'(z) = R(z)/R(Z0) and P'(z) = P(z)/P(Z0). Then

$$\frac{D(z)}{D(Z0)} = \frac{N\ R(z)}{N\ R(Z0)} \frac{\delta(z)}{\delta(Z0)} = R'(z)\frac{\delta(z)}{\delta(Z0)}$$

and also

$$\frac{D(z)}{D(Z0)} = \frac{N' P(z)}{N' P(Z0)} = P'(z).$$

$$R'(z) = \frac{\delta(Z0)}{\delta(z)} P'(z) \qquad (4)$$

Let us now investigate Eq. 3a further. The quantity $P(z-\alpha r)$ may be expanded using a Taylor's series:

$$P(z-\alpha r) = P(z) - \alpha r \frac{dP}{dz} + \frac{(\alpha r)^2}{2!} \frac{d^2P}{dz^2} - \frac{(\alpha r)^3}{3!} \frac{d^3P}{dz^3} + \ldots \qquad (5)$$

where dP/dz etc. are the derivatives of the function P(z) evaluated at depth z. Then, combining Eqs. 3a and 5, the relation between $\delta(z)$ and α becomes:

$$\frac{1}{\delta(z)} = 1 - \alpha r \frac{dP/dz}{P} + \frac{(\alpha r)^2}{2!} \frac{d^2P/dz^2}{P} - \frac{(\alpha r)^3}{3!} \frac{d^3P/dz^3}{P} + \ldots \qquad (6)$$

For small chambers or small gradients, this expression may be approximated by:

$$\delta(z) = 1 + \alpha r \frac{dP/dz}{P} \qquad (6a)$$

The above relation illuminates the meaning of an expression sometimes used[4,7-9] to describe the dependence of δ on the radius of the chamber, viz., δ = 1-(factor) r. This factor may now be identified with $\alpha(dP/dz)/P$ (which is, of course, negative beyond z_{max}) and, as such, it will depend on both chamber geometry and the gradient of the radiation field.

If the measured dose distribution P(z) were purely exponential for all depths, dP/dz etc. would be proportional to P(z). It would then follow from Eq. 6 that $\delta(z)$ will be constant with depth, and so will R'(z)/P'(z), according to Eq. 4. This would imply that, as both curves R'(z) and P'(z) are normalized to unity at a given depth, they will coincide at all depths. In such a case, there would be no way to derive the value of $\delta(z)$ or α from relative measurements only, and one would have to rely on in-air calibrations,[1] with all their inherent uncertainties. However, in most high penetration photon and neutron therapy beams there is a fairly broad region around the depth for maximum dose build-up where D(z) is not exponential.[6,11-13] In these cases, R'(z)/P'(z) is a function of depth and, based on Eqs. 4 and 6, a value for αr may be determined from the relative measurements described above.

Experimental Method.

The p(66)Be(49) neutron beam at the Fermilab Neutron Therapy Facility[14] was used for the measurements. This is a highly penetrating beam with a depth for maximum dose (z_{max}) of about 1.5 cm.[15,16] The depth dose curves for two or three different field sizes and SSDs were measured at depths greater than z_{max} in a tissue equivalent liquid phantom.

Five ionization chambers were used for these measurements. All of them had A-150 tissue equivalent plastic walls[17] and were air filled. They were:

(a) A parallel plate chamber with a 2 cm di ter collector and a 1 mm air gap.[18]

(b) A 0.1 cm^3 thimble chamber,[19] with an inner cavity radius of 0.23 cm

(c) A 0.5 cm^3 thimble chamber,[20U] with an inner cavity radius of 0.45 cm.

(d) A 1.0 cm^3 spherical chamber,[21] with an inner cavity radius of 0.70 cm.

(e) An 8 cm^3 spherical chamber,[D22] with an inner cavity radius of 1.24 cm.

The measurements were made in a phantom consisting of a Lucite tank measuring approximately 3 cm^3, filled with Frigerio's TE-solution[23] of density 1.07 g cm^{-3}. The phantom was not disturbed while changing from one chamber to another, ensuring that identical irradiation conditions were experienced by all chambers. The chambers were clamped to a remotely controlled scanner which could change their position with a precision of better than $\pm$0.5 mm. Each chamber was initially positioned inside the phantom at a reference depth of Z0 = 10.0 cm by means of individually calibrated stainless steel spacers. This positioning had an estimated precision of $\pm$0.5 mm.

The ionization chambers were operated with polarization potentials ranging from +300 V for the 0.1 cm^3 chamber to +900 V for the 8 cm^3 chamber, which insured adequate collection efficiency at all depths for all chambers.[24] The output from all chambers was fed to microcomputer controlled integrators described elsewhere.[25,26] Their collected charges, corrected for temperature and pressure, were normalized to the output of monitor transmission ionization chambers and averaged over several cycles of measurements. Multiple scans were performed with each chamber for each radiation field, and the reproducibility of the readings was better than $\pm$0.5%.

Results and Analysis

The central axis depth doses of two widely different radiation fields were measured with all five chambers: a 7.5 x 7.5 cm^2 field at an SSD of 143 cm and a 35 cm diameter field (side of equivalent square = 31 cm) at an SSD of 180 cm. In addition, the parallel plate and spherical chambers were used to scan a 12 x 12 cm^2 field at an SSD of 190 cm. These field sizes and SSDs afforded a range of depth dose gradients with which to test the hypothesis of a gradient dependent displacement correction factor. The readings of each chamber for each field size were normalized to unity at the reference depth of Z0 = 10 cm.

In order to interpolate more precisely between the measured points, a quadratic polynomial of the form $\ln[R(z)] = az^2 + bz + c$ was fitted through four points at a time such that there were two data points at either side of each interpolation region. This interpolation method was chosen instead of an analytical function fit used in an earlier report[15] to avoid prejudging the form of the depth dose curve and possibly biasing subsequent analyses. As it would be expected, the fits to the data points are very good; however, this method introduces discontinuities every time the set of four points used to define the polynomial is changed by "sliding" along the depth dose curve. These artifacts tend to increase the noise when ratios or derivatives are taken, as shown in Figs. 2 through 4.

The normalized depth dose curves measured with the PPIC for the two extreme field sizes are shown in the upper part of Fig. 2 together with the corresponding fits. The logarithmic derivatives $(dP/dz)/P(z)$ of the calculated polynomial fits are shown in the lower part of Fig. 2. As mentioned, discontinuities in slope hardly visible in the depth dose fits are enhanced in the gradient plots. This figure shows that $(dP/dz)/P(z)$ is changing rapidly with depth up to about 10 cm, but becomes almost constant at larger depths.

The differences in the depth dose curves measured with different chambers are shown in Fig. 3. In the upper portion of Fig. 3(a), the curves measured with the PPIC and the 8 cm^3 chamber for the 7.5 x 7.5 cm^2 field size are shown together with their respective fits. While the two curves coincide at at depth of 10 cm because of normalization, they are seen to diverge elsewhere, especially at smaller depths. This can be seen more clearly in the lower portion of Fig. 3(a), where the ratios R'(z)/P'(z) of normalized readings, as calculated from the polynomial fits to each set of measurements, are plotted for all four practical chambers. Clearly, these ratios deviate significantly from unity at depths smaller than the reference depth, albeit at different rates depending on the dimensions of the chambers. The deviations from unity of some ratios at the reference depth of 10 cm (on the order of 0.2%) are a measure of the uncertainties introduced by the polynomial fits. Fig. 3(b) shows the very similar results obtained for the 35 cm diameter field size.

According to Eq. 4, R'(z)/P'(z) is inversely proportional to $\delta(z)$. It appears, therefore, that the "displacement factor" δ is indeed a function of depth or, more precisely, of the logarithmic gradient of the depth dose curve, which is changing with depth as seen in Fig. 2.

By substituting Eq. 6 or 3a in Eq. 4, it may be seen that the relationship between the normalized measured functions R'(z) and P'(z) involves only one adjustable parameter, namely αr (or α, if r is known), since all the derivatives of P(z) are determined by measurement. The least-squares-fit value of this parameter was determined for each chamber and each field size by means of a non-linear minimization routine available on the Fermilab computers.[27] The polynomial fit to the normalized parallel plate measurements, P'(z), as well as its derivatives, were stored for each field size. An initial arbitrary value of αr was used in Eq. 6 to calculate $\delta(z)$ and $\delta(Z0)$ for each of the other chambers at all measured depths. The displaced values predicted from Eq. 4 $[P'(z)\ \delta(Z0)/\delta(z)]$ were then compared to the measured normalized readings, R'(z). The least-squares-fit values of αr for each chamber were determined by minimizing the resulting χ^2 values.

The results of the fitting procedures are summarized in Table 1 and in Fig. 4. For each chamber and field size, the value of αr that gave the best correction to the chamber readings with respect to the PPIC results is shown in Table 1, together with the value of α derived from measured chamber dimensions. Also given in Table 1 are the values of $\delta(z)$ evaluated at z = 10 cm using Eq. 6. The functions $\delta(z)$ appropriate for the 5 X 7.5 cm^2 and 35 cm diameter fields, calculated using Eq. 6 and the adopted values of αr from Table 1, are shown in Fig. 4 (a) and 4 (b), respectively, for all four practical chambers.

As a check, new fits to the depth doses measured with each chamber and field size were calculated by multiplying the function P'(z), from Fig. 2, by the factors $\delta(Z0)/\delta(z)$ obtained by using Eq. 6 and the optimum values for αr from Table 1. These fits were almost as good as the original ones, although small deviations from the data were discernible at larger depths.

Discussion

Although the measurements presented in this work were restricted to depths greater than that for maximum dose, the present approach is valid in the build-up region, too.[6] In fact, a corollary of Eq. 6 is that, if an ionization chamber is placed in a region where the radiation field due to a single source has a null gradient over a range not smaller than the size of the chamber, then the displacement correction factor is unity. This corollary also holds for extended or multiple sources of radiation, provided a plane can be defined that completely separates the radiation sources from the gradient-free region. Furthermore, Eq. 3 still holds in such a region, since the doses at the "effective point of measurement" and at the center of the ionization chamber are equal.

The uncertainties quoted in Table 1 for the adjustable parameter αr come mainly from depth position uncertainties of each chamber relative to the PPIC, from charge measurement uncertainties and from error estimates of the fitting procedures. Because of the small dimensions of the thimble chambers, however, this ± 1 mm uncertainty becomes a large uncertainty in the estimated value of α, the fraction of the radius by which the effective point of measurement has to be moved upstream of the center of the chamber. The consistently higher values of αr determined from the measurements using the 35 cm diameter field size may have arisen from a misplacement of the parallel plate chamber in one of the fields, affecting the analysis of all chambers about equally. The magnitudes of these differences are consistent with the above positioning uncertainty.

The possibility exists, however, that these differences may be due to a real dependence of α on field gradient or on changes in beam quality with field size, arising from different proportions of primary and scattered radiation.[5] Based on the present results, such a dependence would be in the direction of making α larger for larger field sizes. This would compensate in Eq. 6 for the decreasing field gradient, and would tend to make $\delta(z)$ less dependent on field size. This hypothesis was investigated by measuring the central axis depth dose of the intermediate field size, 12 x 12 cm^2. The results obtained with the 1.0 cm^3 chamber are inconclusive, but the value of αr obtained

for the 8 cm^3 chamber deviates sufficiently from a monotonic trend to make such a dependence unlikely.

The spread in the values of α shown in Table 1 makes comparisons with theory inconclusive. The grand average of the derived values for the two thimble chambers is $\alpha = 0.65 \pm 0.3$, while for the two spherical chambers the corresponding average is $\alpha = 0.85 \pm 0.1$. With these large uncertainties, the present results cannot discriminate between predicted values of α,[3,5] but they are not inconsistent with them or with experimentally measured values.[7,28]

The values of $\delta(z)$ shown in Table 1 were evaluated at 10 cm deep because this is the depth at which the depth doses become almost exponential (Fig. 2), and therefore $\delta(z)$ becomes almost constant (Fig. 4). This is also the depth at which routine beam calibrations are performed at Fermilab. The calculated values of $\delta(10)$ for the IC-18 and IC-17 chambers agree very well with the results obtained in a d(35)Be neutron beam by Shapiro et al.,[1] which have been adopted by the AAPM task group on neutron dosimetry.[29] Shapiro et al.[1] also measured dose ratios for the above two chambers at several depths and concluded that there was no depth dependence of their displacement factors. Since the central axis depth dose curves for their beam also display broad regions of non-exponential decrease,[12,13] the present analysis would predict variations of δ with depth, in disagreement with their conclusions.

Conclusions

It has been shown that the two approaches to calculating the correction to ionization chamber readings due to displacement of the phantom material, the "effective point of measurement" and the "displacement correction factor" methods, can be reconciled if the former is assumed to be a constant fraction of the chamber radius and the latter is made a function of the local field gradient. A simple analytical relationship has been presented relating the two quantities.

Measurements of the central axis depth dose of a p(66)Be(49) neutron therapy beam made using different chambers have shown the above assumptions to hold true. The analytical relationship derived in this work was successfully applied to obtain the magnitudes of the corrections for the chambers employed without recourse to in-air calibrations.

The "displacement correction factors" for the commonly used IC-17 and IC-18 TE plastic ionization chambers obtained in this work agree with recommended values,[29] when they are evaluated at depths where the depth dose curves are nearly exponential.

Recommendations

Because the "displacement correction factor" depends on field gradient, its use is not recommended in radiation fields where the logarithmic derivative of the dose changes rapidly with depth. In view of the broad transition region of non-exponential depth dose experienced in penetrating photon and neutron beams, it is recommended that relative dose distribution measurements be made with as small a chamber as possible, to minimize the variations in displacement corrections arising from the changing field gradient. Moreover, absolute dose measurements with calibrated, and presumably larger, ionization chambers should be performed at depths where the variations of the logarithmic field gradient are minimal. For the more penetrating beams these depths could well be much deeper than the 5 cm recommended in the "Code of Practice".[30]

Acknowlegement.

This investigation was supported by PHS Grant Number 5PO1CA18081-07, awarded by the National Cancer Institute, DHHS. The authors would like to thank Michelle Gleason for her untiring efforts in preparing this manuscript.

REFERENCES

(a). The expression p(66)Be(49) means that 66 MeV protons are incident on a semi-thick target. In this target, protons not undergoing nuclear scattering would lose 49 MeV by ionization. p(66)Be would mean a thick target.

1. Shapiro, P., Attix, F. H., August, L. S., Theus, R. B., Rogers, C. C., Displacement Correction Factor for Fast-Neutron Dosimetry in a Tissue-Equivalent Phantom, Med. Phys. 3, 87 (1976).

2. Holt, J. G., Fleischman, R. C., Perry, D. J., Buffa, A., Examination of the Factors A_c and A_{eq} for Cylindrical Chambers Used in Cobalt-60 Beams, Med. Phys. 6, 280 (1979).

3. Burlin, T. E., On the Point of Dose Measurement with Ionization Chambers in a Phantom Irradiated by Neutron Beams, in "Ion Chambers for Neutron Dosimetry", Broerse, J. J., editor, Harwood Academic Publishers: New York, 1980. p. 281.

4. Zoetelief, J., Engels, A. C., Broerse, J. J., Displacement Correction Factors for Spherical Ion Chambers in Phantoms Irradiated with Neutrons of Different Energies, Phys. Med. Biol. 26, 513 (1981).

5. Dutreix, A., Effective Point of Measurement for In-Phantom Measurements with Protons, in "Ion Chambers for Neutron Dosimetry", Broerse, J. J., editor, Harwood Academic Publishers: New York, 1980. p. 259.

6. Hettinger, G., Pettersson, C. and Svensson, H., Displacement Effect of Thimble Chambers Exposed to a Photon or Electron Beam from a Betatron, Acta Radiologica 6, 61 (1967).

7. Zoetelief, J., Engels, A. C., Broerse, J. J. and Mijnheer, B. J., Effect of Finite Size of Ion Chambers Used for Neutron Dosimetry, Phys. Med. Biol. 25, 1121 (1980).

8. Zoetelief, J., Engels, A. C., Broerse, J. J., Effective Measuring Point of Ion chambers for Photon Dosimetry in Phantoms, Br. J. Radiol. 53, 580 (1980).

9. Williams, J. R., Ryall, R. E., Bonnett, D. E., Measurements of Displacement Factors in a Neutron Beam Using Activation Dosemeters, Phys. Med. Biol. 27, 81 (1982).

10. Mijnheer, B. J., Broers-Challiss, J. E., Broerse, J. J., in Proceedings of 2nd Symposium on Neutron Dosimetry in Biology and Medicine, Burger, G., and Ebert, H. G., editors, Luxembourg, CEC 1975. p. 423.

11. Ten Haken, R. K., Awschalom, M., Hendrickson F., Rosenberg, I., Comparison of the Physical Characteristics of a p(66)Be(49) Neutron Therapy Beam to Those of Conventional Radiotherapy Beams, Fermilab Internal Report TM-1021R, December 1980.

12. Almond, P. R., Smathers, J. B., Oliver, G. D., Jr., Hranitzky, E. B., Routt, K., Dosimetric Properties of Neutron Beams Produced by 16-60 MeV Deuterons on Beryllium, Radiation Research 54, 24 (1973).

13. Shapiro, P., August, L. S., Theus, R. B., Computer Generation of Dose Distributions for a Fast-Neutron Therapy Beam, Med. Phys. 6, 12 (1979).

14. Cohen, L., Awschalom, M., The Cancer Therapy Facility at the Fermi National Accelerator Laboratory, Batavia, Illinois, a Preliminary Report, Applied Radiol. 5, 51 (1976).

15. Rosenberg, I., Awschalom, M., Characterization of a p(66)Be(49) Neutron Therapy Beam: I. Central Axis Depth Dose and Off-Axis Ratios, Med. Phys. 8, 99 (1981).

16. Awschalom, M., Rosenberg, I., Characterization of a p(66)Be(49) Neutron Therapy Beam. II. Skin-Sparing and Dose Transition Effects, Med. Phys. 8, 105 (1981).

17. Smathers, J. R., Otte, V. A., Smith. A. R., Almond, P. R., Attix, F. H., Spokas, J. J., Quam, W. M., Goodman, L. J., Composition of A-150 Tissue-Equivalent Plastic, Med. Phys. 4, 74 (1977).

18. Rosenberg, I., Awschalom, M., Ten Haken, R. K., The Effect of Missing Backscatter on the Dose Distribution of a p(66)Be(49) Neutron Therapy Beam, Med. Phys. 9, 559 (1982).

19. E G & G, Model IC-18, now available from Far West Technologies, Inc., Goleta, CA. 93017

20. Exradin, Model T-2, Warrenville, IL. 60555

21. E G &G, Model IC-17, now available from Far West Technologies, Inc., Goleta, CA. 93017

22. Designed and built at the University of Wisconsin.

23. Frigerio, N. A., Coley, R. F., Simpson, M. J., Depth Dose Determination I. Tissue Equivalent Liquids for Standard Man and Muscle, Phys. Med. Biol. 17, 792 (1972).

24. Awschalom, M., Rosenberg, I., Ten Haken, R. K., Pearson, D. W., Attix, F. H., DeLuca, P. M., Characteristics of A-150 Plastic-Equivalent Gas in A-150 Plastic Ionization Chambers for

p(66)Be(49) Neutrons, to appear in Med. Phys.

25. Awschalom, M., Rosenberg, I., Neutron Beam Calibration and Treatment Planning, Fermilab Internal Report TM-834, December 1978.

26. Awschalom, M., Goodwin, R., Grumboski, Rosenberg, I., Shea, M., High Precision in Dose Delivery: Routine Use of a Microcomputer, in "Biomedical Dosimetry: Physical Aspects, Instrumentation, Calibration", Vienna, IAEA 1981.

27. "MINUIT" Multivariable minimization program from CERN Computing Facility, Geneva, Switzerland.

28. Johansson, K. A., Mattsson, L. O., Lindborg, L., Svensson, H., National and International Standardization of Radiation Dosimetry, STI/PUB/471, Vol. II, Vienna: IAEA (1978) p. 243.

29. American Association of Physicists in Medicine Report No. 7, Protocol for Neutron Beam Dosimetry, New York: American Institute of Physics, 1980.

30. American Association of Physicists in Medicine, Code of Practice for X-Ray Therapy Linear Accelerators, Med. Phys. 2, 110 (1975).

Table Captions

Table 1. Summary of Calculated α and δ Factors.

Notes:

αr: radial displacement necessary to reconcile the relative depth dose measurements of each chamber with those of the parallel plate chamber for each field size, determined from least-squares fits.

$\delta(10)$: displacement correction factor evaluated at 10 cm deep using Eq. 6 in the text and the corresponding value of αr.

$(dP/dz)/P$: logarithmic derivative calculated from the fits to the depth dose data measured with the parallel plate chamber, evaluated at 10 cm deep.

Table 1

Summary of Calculated α and δ Factors

Chamber	IC-18 ($0.1cm^3$)			Exradin ($0.5cm^3$)			IC-17 ($1cm^3$)			U of W ($8\ cm^3$)			$\frac{dP/dz}{P}$
Shape	Thimble			Thimble			Spherical			Spherical			
Inner Radius	r = 0.23 cm			r = 0.45 cm			r = 0.70 cm			r = 1.24 cm			evaluat at z=10
Field Sizes and SSD	αr (cm)	α	$\delta(10)$	αr (cm)	α	$\delta(10)$	αr (cm)	α	$\delta(10)$	αr (cm)	α	$\delta(10)$	(cm^{-1})
5 x 7.5 cm^2 SSD = 143 cm	0.10 $\pm$0.1	0.44 $\pm$0.4	0.994 $\pm$.006	0.26 $\pm$0.1	0.58 $\pm$0.2	0.984 $\pm$.006	0.49 $\pm$0.1	0.70 $\pm$0.1	0.970 $\pm$.006	1.12 $\pm$0.1	0.90 $\pm$0.1	0.933 $\pm$.006	$\pm$ -0.06
x 12 cm^2 SSD = 190 cm	-	-	-	-	-	-	0.58 $\pm$0.1	0.83 $\pm$0.1	0.971 $\pm$.005	1.00 $\pm$0.1	0.81 $\pm$0.1	0.950 $\pm$.005	-0.052
cm diam. SSD = 180 cm	0.18 $\pm$0.1	0.79 $\pm$0.4	0.992 $\pm$.004	0.35 $\pm$0.1	0.78 $\pm$0.2	0.985 $\pm$.004	0.61 $\pm$0.1	0.87 $\pm$0.1	0.974 $\pm$.004	1.18 $\pm$0.1	0.96 $\pm$0.1	0.951 $\pm$.004	-0.043
α from Dutreix	-	0.85	-	-	0.85	-	-	0.75	-	-	0.75	-	Ref. 5
α from Hettinger	-	0.75	-	-	0.75	-	-	-	-	-	-	-	Ref. 6
δ from Shapiro	-	-	0.989	-	-	-	-	-	0.970	-	-	-	Ref. 1

Figure Captions

Fig. 1. Corrections to cavity ionization chamber readings due to displacement of the medium. Both the "effective point of measurement" and "displacement factor" methods are illustrated.

Fig. 2. Upper: Central axis depth doses for two field sizes, measured with the parallel plate chamber. The symbols are data. The curves represent interpolated fits described in the text. The results were normalized to unity at 10 cm deep in each case.

Lower: Logarithmic derivatives of the above curves as a function of depth. Sharp changes in the curves arise from discontinuities in the interpolation procedures.

Fig. 3(a). Upper: Central axis depth doses for the 5 x 7.5 cm^2 field size, as measured with the parallel plate chamber (A) and the 8 cm^3 chamber (E). The symbols are data. The curves represent interpolated fits described in the text. The results were normalized to unity at 10 cm deep in each case.

Lower: Ratios of normalized depth dose curves to parallel plate chamber results (A), as a function of depth. Curves are shown for: (B) 0.1 cm^3 chamber; (C) 0.5 cm^3 chamber; (D) 1.0 cm^3 chamber; and (E) 8 cm^3 chamber. Sharp changes in the curves arise from discontinuities in the interpolation procedures.

Fig. 3(b). As for Fig. 3(a), but for 35 cm diameter field size.

Fig. 4(a). Displacement correction factors, $\delta(z)$, as a function of depth, derived from the measurements with the 7.5 x 7.5 cm^2 field size. The functions were calculated from Eq. 6 in the text, using the gradients of the interpolated fits to the parallel plate chamber measurements (Fig. 2) and the corresponding least-squares-fit values of αr (Table 1). Curves are shown for: (B) 0.1 cm^3 chamber; (C) 0.5 cm^3 chamber; (D) 1.0 cm^3 chamber; and (E) 8 cm^3 chamber.

Fig. 4(b): As for Fig. 4(a), but for 35 cm diameter field size.

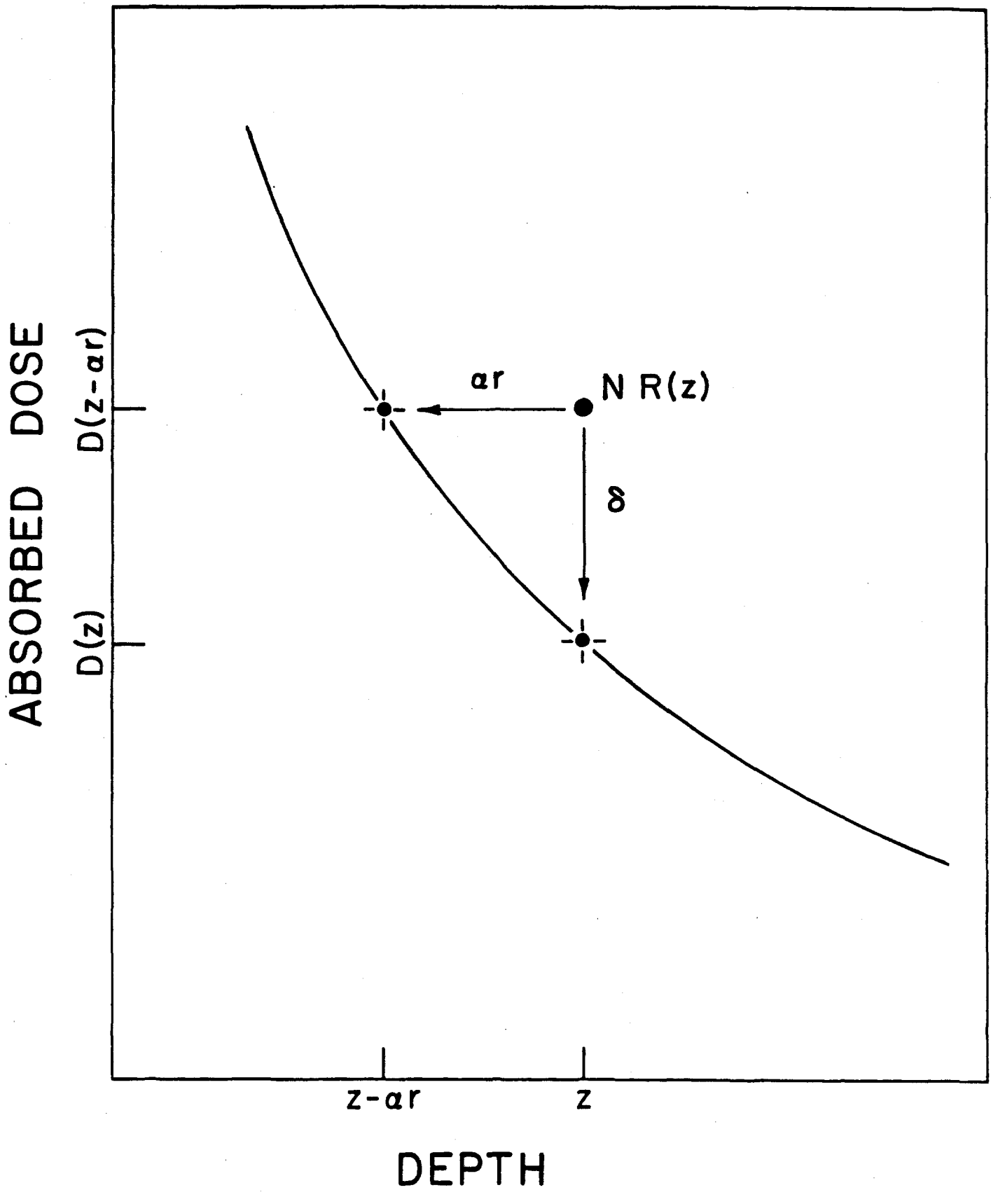

Figure 1

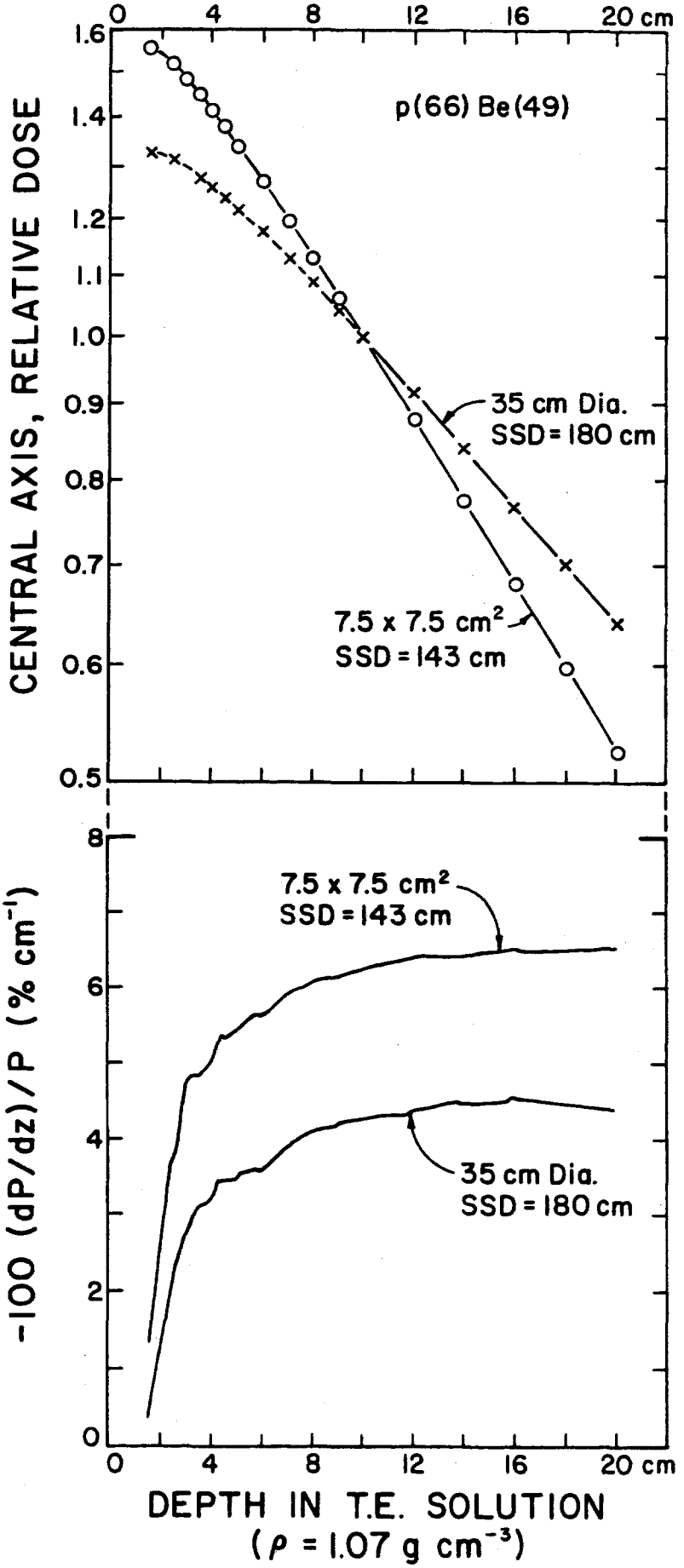
0
4
8
12
16
20 cm
1.6
1.4
1.2
1.1
1.0
0.9
0.8
0.7
0.6
0.5
CENTRAL AXIS, RELATIVE DOSE
p(66) Be(49)
35 cm Dia.
SSD = 180 cm
7.5 x 7.5 cm²
SSD = 143 cm
8
6
4
2
0
-100 (dP/dz)/P (% cm⁻¹)
7.5 x 7.5 cm²
SSD = 143 cm
35 cm Dia.
SSD = 180 cm
0
4
8
12
16
20 cm
DEPTH IN T.E. SOLUTION
(ρ = 1.07 g cm⁻³)

Figure 2

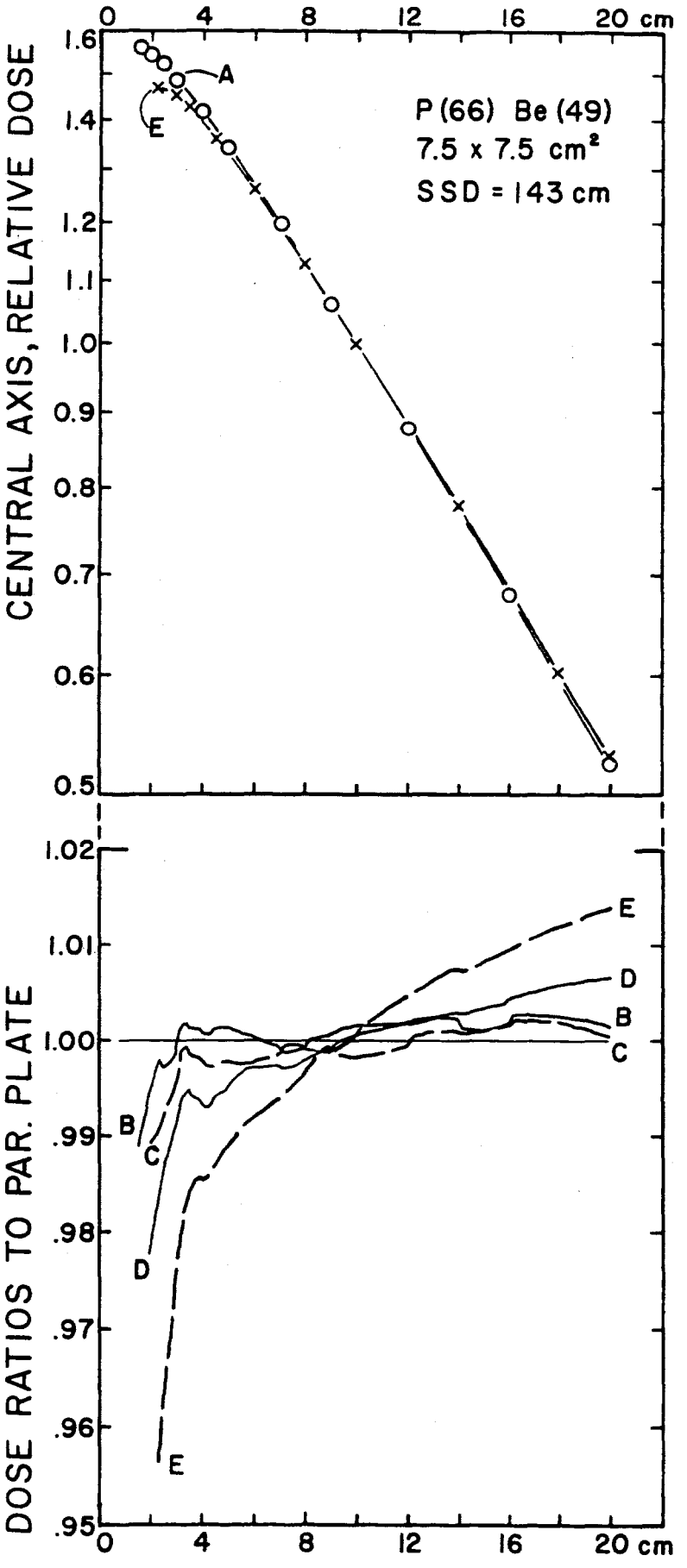
0 4 8 12 16 20 cm
1.6
1.4
1.2
1.1
1.0
0.9
0.8
0.7
0.6
0.5
CENTRAL AXIS, RELATIVE DOSE
A
E
P(66) Be(49)
7.5 x 7.5 cm²
SSD = 143 cm
1.02
1.01
1.00
.99
.98
.97
.96
.95
DOSE RATIOS TO PAR. PLATE
B
C
D
E
0 4 8 12 16 20 cm
DEPTH IN T.E. SOLUTION

Figure 3(a)

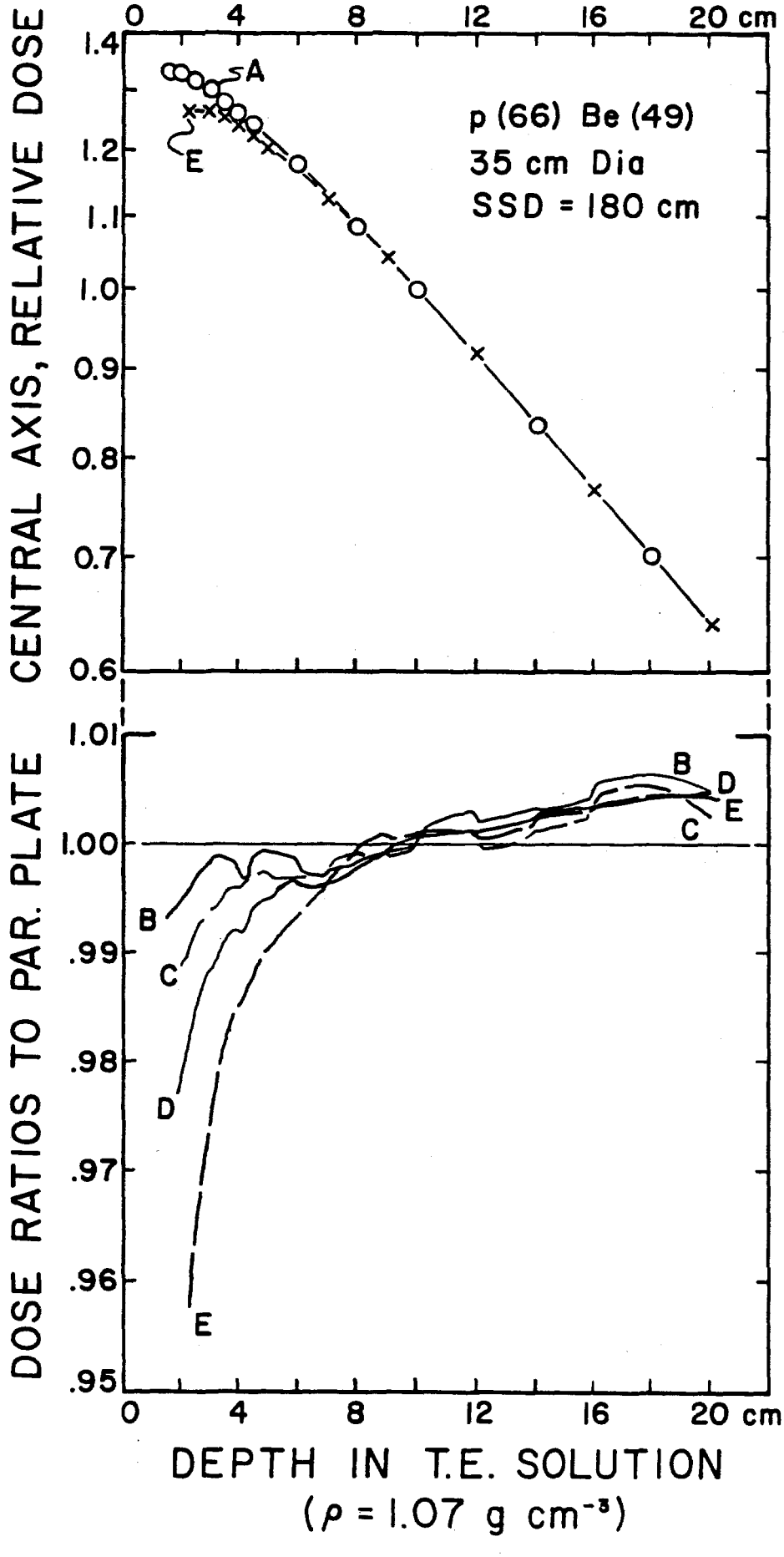
0 4 8 12 16 20 cm
1.4
1.2
1.1
1.0
0.9
0.8
0.7
0.6
A
E
p (66) Be (49)
35 cm Dia
SSD = 180 cm
CENTRAL AXIS, RELATIVE DOSE
1.01
1.00
.99
.98
.97
.96
.95
B
D
E
C
B
C
D
E
DOSE RATIOS TO PAR. PLATE
0 4 8 12 16 20 cm
DEPTH IN T.E. SOLUTION
(ρ = 1.07 g cm⁻³)

Figure 3(b)

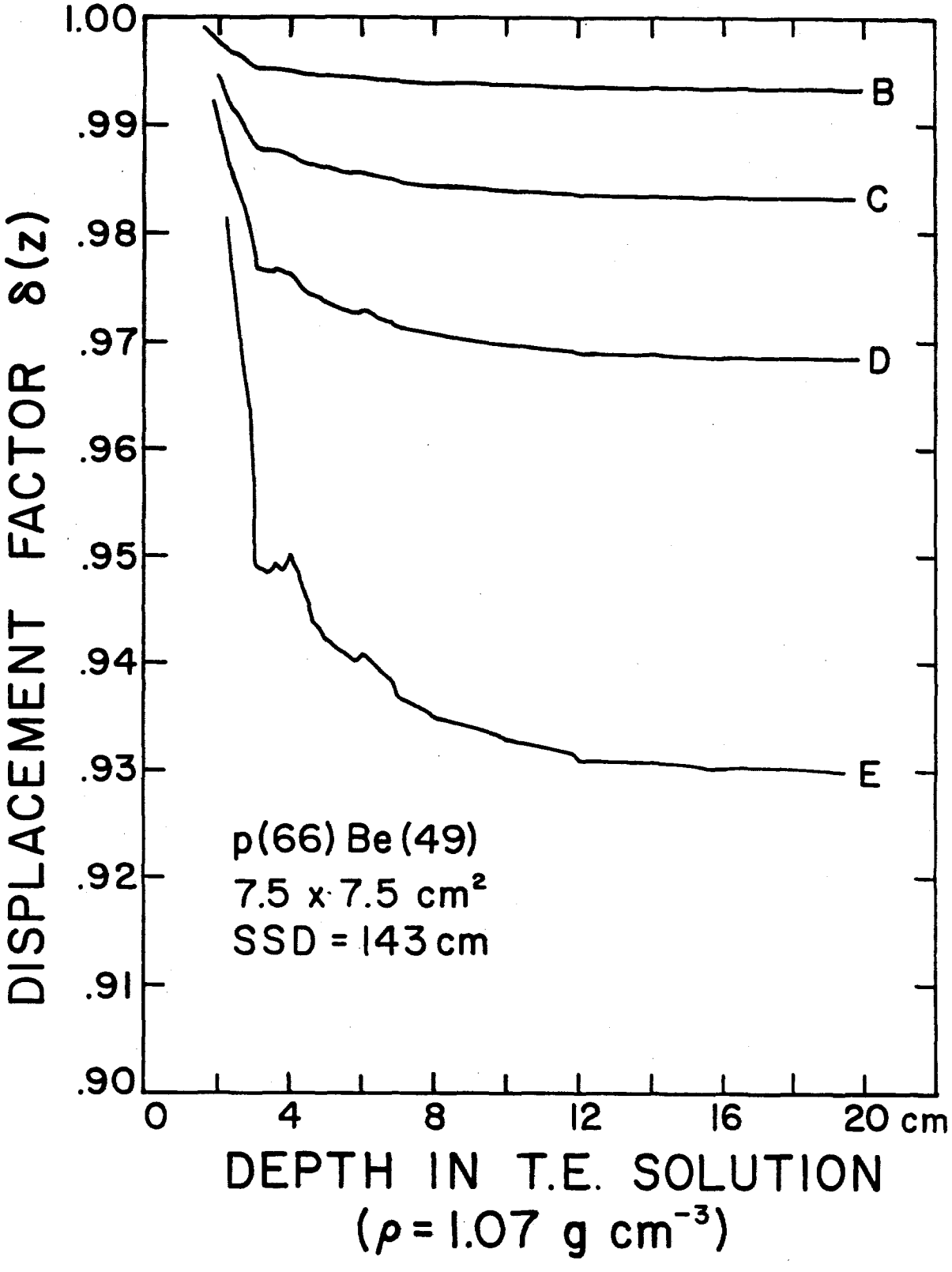
1.00
.99
.98
.97
.96
.95
.94
.93
.92
.91
.90
DISPLACEMENT FACTOR δ(z)
B
C
D
E
p(66) Be(49)
7.5 x 7.5 cm²
SSD = 143 cm
0
4
8
12
16
20 cm
DEPTH IN T.E. SOLUTION
(ρ = 1.07 g cm⁻³)

Figure 4(a)

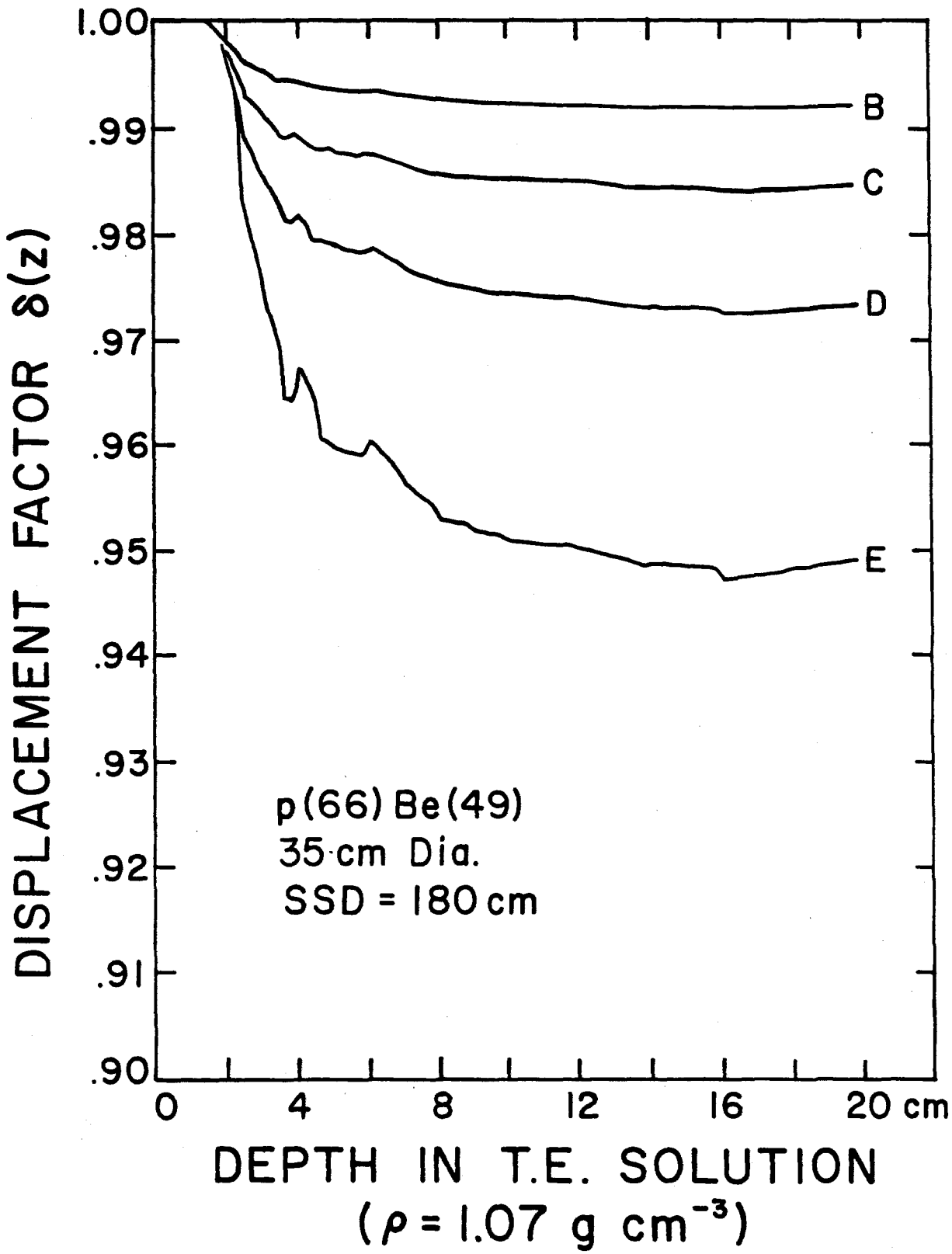
1.00
.99
.98
.97
.96
.95
.94
.93
.92
.91
.90
DISPLACEMENT FACTOR δ(z)
B
C
D
E
p(66) Be(49)
35 cm Dia.
SSD = 180 cm
0
4
8
12
16
20 cm
DEPTH IN T.E. SOLUTION
(ρ = 1.07 g cm⁻³)

Figure 4(b)